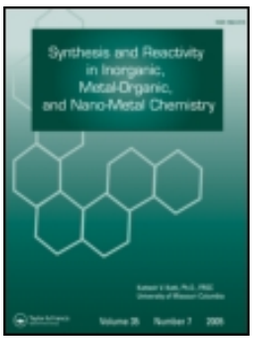

Taylor & Francis
Taylor & Francis Group

Synthesis and Reactivity in Inorganic, Metal-Organic, and Nano-Metal Chemistry

ISSN: 1553-3174 (Print) 1553-3182 (Online) Journal homepage: https://www.tandfonline.com/loi/lsrt20

Adsorption and Inhibitor Action of 4-(N,N-Dimethylamino) Benzaldehyde Thiosemicarbazone on 6061 Al/SiC Composite and its Base Alloy in Sulfuric Acid Medium

Geetha Mable Pinto , Jagannath Nayak & A. Nityananda Shetty

To cite this article: Geetha Mable Pinto , Jagannath Nayak & A. Nityananda Shetty (2011) Adsorption and Inhibitor Action of 4-(N,N-Dimethylamino) Benzaldehyde Thiosemicarbazone on 6061 Al/SiC Composite and its Base Alloy in Sulfuric Acid Medium, Synthesis and Reactivity in Inorganic, Metal-Organic, and Nano-Metal Chemistry, 41:2, 127-140, DOI: 10.1080/15533174.2010.538023

To link to this article: https://doi.org/10.1080/15533174.2010.538023

Synthesis and Reactivity in Inorganic, Metal-Organic, and Nano-Metal Chemistry, 41:127–140, 2011

ISSN: 1553-3174 print / 1553-3182 online
DOI: 10.1080/15533174.2010.538023

Taylor & Francis
Taylor & Francis Group

Adsorption and Inhibitor Action of 4-(N,N-Dimethylamino) Benzaldehyde Thiosemicarbazone on 6061 Al/SiC Composite and its Base Alloy in Sulfuric Acid Medium

Geetha Mable Pinto,[1] Jagannath Nayak,[2] and A. Nityananda Shetty[1]

[1]*Department of Chemistry, National Institute of Technology Karnataka, Srinivasnagar, India*
[2]*Department of Metallurgical and Materials Engineering, National Institute of Technology Karnataka, Srinivasnagar, India*

The inhibitive action of 4-(N,N-dimethylamino)benzaldehyde thiosemicarbazone (DMABT) on the corrosion behavior of 6061 Al -15 vol. pct. SiC(p) composite and its base alloy was studied at different temperatures in sulfuric acid medium containing varying concentrations of it, using Tafel extrapolation technique and AC impedance spectroscopy (EIS). Results showed that DMABT was an effective inhibitor, showing inhibition efficiency of 70% in 0.5 M sulfuric acid. The adsorption of DMABT on both the composite and base alloy was found to be through physisorption obeying Langmuir adsorption isotherm. The thermodynamic parameters such as free energy of adsorption and activation parameters were calculated.

Keywords acid corrosion, aluminum, EIS, metal matrix composites, polarization

INTRODUCTION

Aluminium matrix composites (AMCs) have received considerable attention for military, automobile, and aerospace applications because of their low density, high strength, and high stiffness.[1–6] Further, the addition of ceramic reinforcements (SiC) has raised the performance limits of the Al (6061) alloys.[7] It is known that aluminium matrix composites exhibited better resistance to mechanical wear than their base alloys and hence they have specific strength for numerous weight sensitive applications.[8–9] One of the main disadvantages in the use of metal matrix composite is the influence of reinforcement on corrosion rate. The addition of a reinforcing phase could lead to discontinuities in the film, thereby increasing the number of sites where corrosion can be initiated and thereby making the composites more susceptible for corrosion.[8,10] However the high corrosion rates of these composites, particularly in acid media, can be combated using inhibitors.[11–12] A wide variety of compounds have been used as inhibitors for aluminum and its alloys in acid media. These are mainly organic compounds containing N, S, or O atoms[13–16] and critical use of these compounds in industries has also been reviewed.[17–19] Owing to their usefulness in several stages of process industries, organic compounds containing both N and S atoms function as better adsorption inhibitors because of their lone pair of electrons and polar nature of the molecules.[20–21] Thiosemicarbazone and their derivatives have continued to be the subject of extensive investigation in chemistry and biology owing to their broad spectrum of anti tumor activity,[22] and in many other applications including corrosion and inhibition of metals.[23]

The present work aims at investigating the inhibitive action of 4-(N,N-dimethylamino)benzaldehyde thiosemicarbazone(DMABT) on the corrosion behavior of 6061 Al-15 vol. pct. SiC(p) composite and its base alloy in sulfuric acid solutions at different concentration levels of the acids as well as at different temperatures. Sulfuric acid solution is used for pickling, chemical, and electrochemical etching and in many chemical process industries where aluminum composites are used. The study of corrosion behavior and control of corrosion of the base alloy and the composite in sulfuric acid solution is particularly useful in the field where metal matrix composite is exposed to the corrosion environment containing sulfuric acid. DMABT with the presence of electronegative elements like nitrogen and sulfur and also the π electrons on the benzene ring is expected to be capable of strongly getting adsorbed on the metal surfaces. The bulkiness of the molecule may provide a good surface coverage. Both the above factors would result in a better corrosion inhibition by the compound.

EXPERIMENTAL

Material

The experiments were performed with specimens of 6061 Al-15 vol. pct. SiC(p) composite and its base alloy in extruded rod

Received 14 May 2010; accepted 18 August 2010.
Address correspondence to A. Nityananda Shetty, Department of Chemistry, National Institute of Technology Karnataka, Srinivasnagar – 575 025, India. E-mail: nityashreya@gmail.com

TABLE 1
The composition of the base metal Al 6061 alloy

Element	Cu	Si	Mg	Cr	Al
Composition (Wt.%)	0.25	0.6	1.0	0.25	Bal

form (extrusion ratio 30:1). The composition of the base metal 6061 Al alloy is given in Table 1. Cylindrical test coupons were cut from the rods and sealed with epoxy resin in such a way that the areas of the composite and the base alloy exposed to the medium were 0.95 cm^2 and 0.785 cm^2, respectively. These coupons were polished as per standard metallographic practice, belt grinding followed by polishing on emery papers, and finally on polishing wheel using levigated alumina to obtain mirror finish. It was then degreased with acetone, washed with double distilled water, and dried before immersing in the corrosion medium.

Medium

Standard solution of sulfuric acid was prepared from analytical grade (Nice) acids. The three solutions used for the study were with the following concentrations of sulfuric acid: 0.5 M, 0.25 M and 0.05 M. Experiments were carried out using calibrated thermostat at temperatures 30°C, 35°C, 40°C, 45°C, 50°C (±0.5°C). The inhibitive effect was studied by introducing 50 ppm to 400 ppm (0.2 mM to 1.6 mM) of DMABT into sulfuric acid solutions.

Electrochemical Measurements

Tafel polarization studies

Electrochemical measurements were carried out by using an electrochemical work station, Auto Lab 30, and GPES software. Tafel plot measurements were carried out using conventional three electrode Pyrex glass cell with platinum counter electrode and saturated calomel electrode (SCE) as reference electrode. All the values of potential are therefore referred to the SCE. Finely polished composite and base alloy specimens were exposed to corrosion medium of different concentrations of sulfuric acid at different temperatures (30°C to 50°C) and allowed to establish a steady state open circuit potential. The potentiodynamic current-potential curves were recorded by polarizing the specimen to -250 mV cathodically and +250 mV anodically with respect to open circuit potential (OCP) at scan rate of 1 mV s^{-1}.

Electrochemical impedance spectroscopy studies (EIS)

The corrosion behaviors of the specimens of the composite and the base alloy were also obtained from EIS technique using electrochemical work station, Auto Lab 30, and FRA software. In EIS technique a small amplitude ac signal of 10 mV and frequency spectrum from 100 kHz to 0.01 Hz was impressed at the OCP and impedance data were analyzed using Nyquist plots. The charge transfer resistance, R_t, was extracted from the diameter of the semicircle in Nyquist plot.

In all the above measurements, at least three similar results were considered and their average values are reported.

Synthesis of 4-(N,N-Dimethylamino)Benzaldehyde Thiosemicarbazone

4-(N,N-Dimethylamino)benzaldehyde thiosemicarbazone was synthesized and recrystallized as per the reported procedure.[24] A mixture containing equimolar ethanolic 4- (N, N-dimethylamino)benzaldehyde and thiosemicarbazone were taken into a round bottom flask. The reaction mixture was refluxed on a hot water bath for about 60 minutes. The light yellow colored product obtained was separated by filtration and dried. The product was recrystallized from ethanol. The recrystallized product was checked by IR spectra, elemental analysis, and melting point.

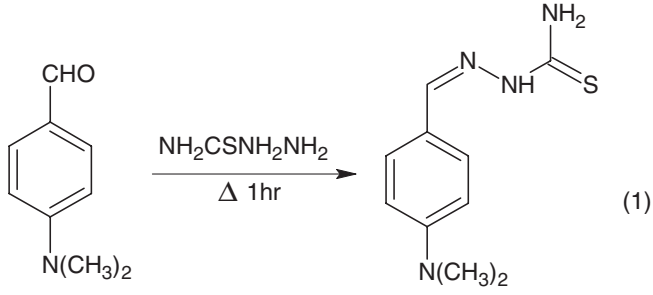

(1)

RESULTS AND DISCUSSION

Potentiodynamic Polarization (PDP) Measurements

The polarization studies of aluminum specimens were carried out in 0.05 M–0.5 M sulfuric acid solutions separately in absence and presence of different concentrations of DMABT. Figures 1 and 2 represents potentiodynamic polarization curve of 6061 Al–SiC composite and its base alloy in 0.5 M sulfuric acid at 30°C solutions in the absence and presence of DMABT. Similar results were obtained in the same concentrations of sulfuric acid at four other temperatures and also in the other two concentrations of the sulfuric acid at the five temperatures studied.

The electrochemical parameters (E_{corr}, i_{corr}, b_a, and b_c) associated with the polarization measurements at different DMABT concentrations for the composite and the base alloy in three different concentrations of the sulfuric acid solution at 30°C are listed in Table 2. The surface coverage θ of the inhibitor on the metal surface is calculated by the expression

$$\theta = i_{corr(uninh)} - i_{corr(inh)} / i_{corr(uninh)} \quad [2]$$

TABLE 2
Electrochemical parameters obtained from potentiodynamic polarization measurements of 6061 Al-SiC composite and its base alloy at various concentrations of DMABT at 30°C

	Composite						Base alloy					
Conc. of H_2SO_4 (M)	Conc. of inhibitor (ppm)	I_{cor} (μA cm^{-2})	-b_c (mV dec^{-1})	b_a (mV dec^{-1})	E_{corr} (mV) (SCE)	IE (%)	Conc. of inhibitor (ppm)	I_{cor} (μA cm^{-2})	-b_c (mV dec^{-1})	b_a (mV dec^{-1})	E_{corr} (mV) (SCE)	IE (%)
0.5	0	91.4	122	59	−597		0	22.9	97	37	−605	
	50	71.2	119	61	−610	22	25	19.0	90	34	−609	17
	100	53.4	117	56	−614	42	50	16.8	91	32	−611	26
	200	40.0	115	55	−615	58	100	13.2	94	30	−615	42
	400	26.7	112	58	−620	71	200	10.9	97	36	−620	52
0.25	0	44.8	88	56	−615		0	17.2	85	28	−622	
	25	35.3	94	54	−621	21	25	14.8	80	26	−625	14
	50	30.7	90	53	−625	31	50	11.8	85	22	−630	31
	100	25.6	95	55	−630	43	100	10.1	84	26	−636	41
	200	16.3	80	49	−629	64						
0.05	0	25.5	70	50	−664		0	9.9	54	20	−679	
	10	21.1	75	49	−667	17	5	8.4	50	17	−683	15
	25	17.8	71	46	−668	30	10	7.5	48	18	−684	24
	50	12.2	74	43	−672	52	25	5.6	51	19	−689	43

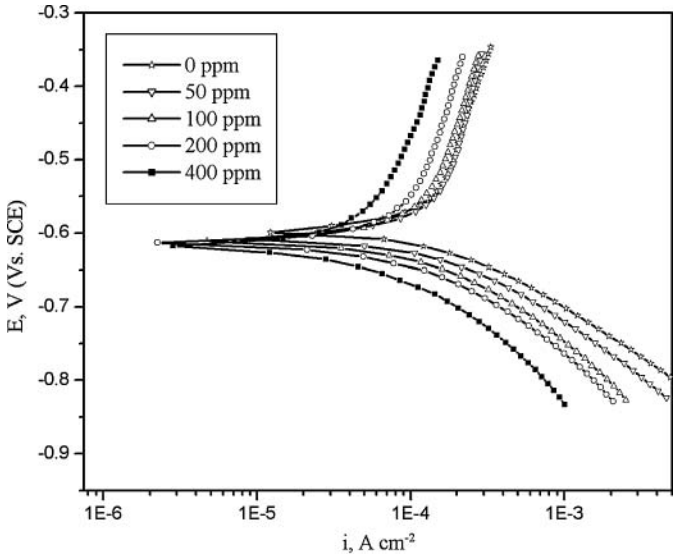

FIG. 1. Tafel curves of 6061 Al- SiC composite in 0.5 M sulfuric acid at 30°C in the presence of different concentrations of DMABT.

The inhibition efficiency (% IE) is calculated by the relation

$$\mathrm{IE}\,(\%) = \theta \times 100 \qquad [3]$$

The data in the table clearly show that the addition of DMABT decreases the corrosion rates of both the composite and the base alloy. Inhibition efficiency increases with increasing DMABT concentration. For the inhibited systems, the values of E_{corr} are shifted to more negative direction and the cathodic branches of the curves are displaced to the left. These are typical features of cathodic inhibitors, in agreement with the results obtained for other aluminum alloys.[25–27]

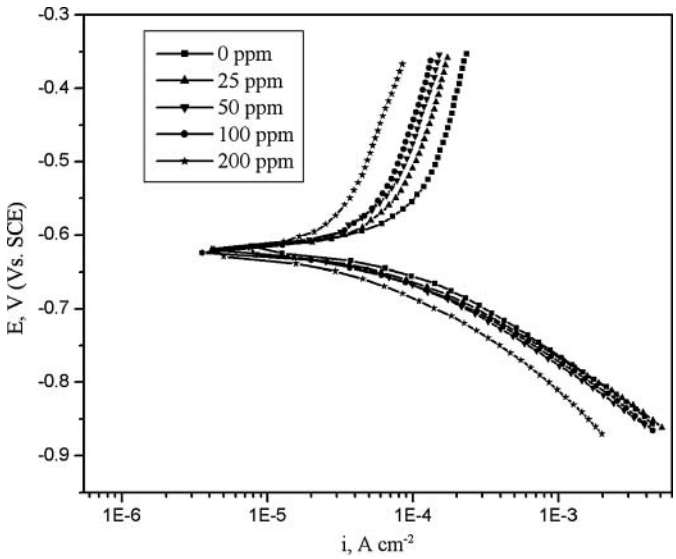

FIG. 2. Tafel curves of 6061 base alloy in 0.5 M sulfuric acid at 30°C in the presence of different concentrations of DMABT.

The anodic and cathodic Tafel slopes remain almost unchanged for the uninhibited and inhibited systems. This indicates that the inhibitive action of DMABT occurs by simple blocking of the available surface area for corrosion attack. In other words, the inhibitor decreased the surface area available for hydrogen evolution without affecting the reaction mechanism and only causes inactivation of part of the surface.[28–29] This fact is an important observation, since the presence of SiC particles in the composite initiate cathodic sites, which is responsible for the higher corrosion of the composite than that of the base alloy.[8,10] Therefore, blocking of these sites via DMABT adsorption would result in decreasing the corrosion rate of composite to a greater extent as compared to the base alloy. The comparison of inhibition efficiency of DMABT for the composite and base alloy at different concentrations and different temperatures shows that the inhibition effect is more on the composite than on the base alloy. The increase in the efficiency of the inhibitor in the case of composite may be due to its heterogenic nature, where the incorporation of silicon carbide acts as the potential active site for the adsorption of the inhibitor. The increase in inhibition efficiency with increasing inhibitor concentration indicates that adsorption of inhibitor molecules increases on the metal surface. Thus, the surface coverage increases as the inhibitor concentration increases.

Electrochemical Impedance Spectroscopy (EIS)

Corrosion behavior of 6061 Al- SiC composite and its base alloy in 0.05 M–0.5 M sulfuric acid solutions, in the absence and presence of different concentrations of DMABT, was also studied by electrochemical impedance spectroscopy. Figures 3 and 4 represent Nyquist plots of 6061 Al – SiC composite and its base alloy, respectively, at various concentrations of DMABT in 0.5 M sulfuric acid at 30°C. Similar results were obtained in two other concentrations of sulfuric acid, and also at other temperatures studied. The electrochemical parameters obtained from the EIS measurements are tabulated in Table 3.

As can be seen from Figures 3 and 4, the impedance diagrams show semicircles, indicating that the corrosion process is mainly charge transfer controlled. In the Nyquist plots for the 6061Al-SiC composite, the impedance spectra consists of a large capacitive loop at high frequencies (HF) and an inductive loop at low frequencies (LF). Similar impedance plots have been reported in literature for the corrosion of pure aluminium and aluminium alloys in various electrolytes such as sodium sulphate,[30–32] sulfuric acid,[31–32] acetic acid,[31,] sodium chloride,[33–34] and hydrochloric acid.[21,29,35–39] The general shape of the curve is similar for all individual samples of the base alloy, with large capacitive loop at high frequencies (HF) and an inductive loop at intermediate frequencies (IF), followed by a second capacitive loop at low frequency (LF) values. Similar results have been reported in literature for the corrosion of pure aluminum in acidic and neutral solutions.[30–31]

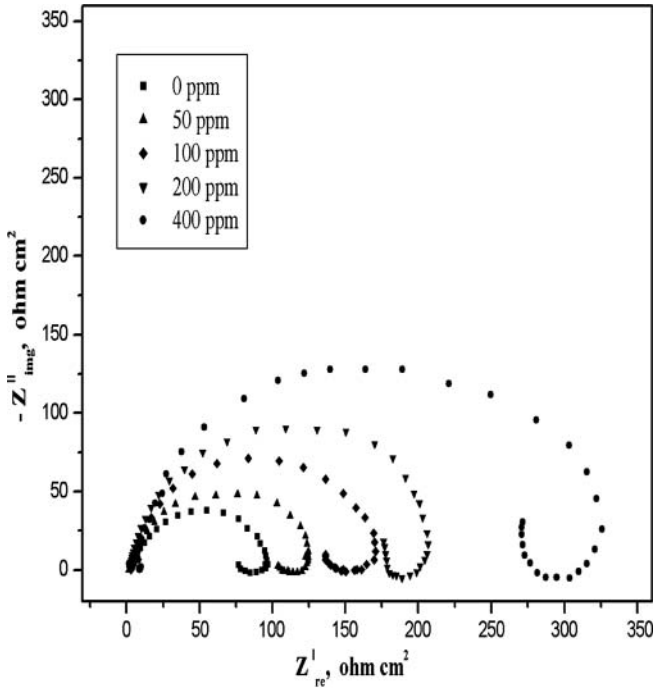

FIG. 3. Nyquist plots of 6061 Al-SiC composite in 0.5 M sulfuric acid at 30°C in the presence of different concentrations of DMABT.

The high frequency capacitive loop could be assigned to the charge transfer of the corrosion process and to the formation of oxide layer.[40−41]. The oxide film is considered to be a parallel circuit of a resistor due to the ionic conduction in the oxide film and a capacitor due to its dielectric properties. According to Brett,[36,38] the capacitive loop is corresponding to the interfacial reactions, particularly the reaction of aluminum oxidation at the metal/oxide/electrolyte interface. The process includes the formation of Al^{+} ions at the metal/oxide interface, and their migration through the oxide/solution interface where they are oxidized to Al^{3+}. At the oxide/solution interface, OH^{-} or O^{2-} ions are also formed. The fact that all the three processes are represented by only one loop could be attributed either to the overlapping of the loops of processes, or to the assumption that one process only dominates, excluding the other processes.[34−35] The other explanation offered to the high frequency capacitive loop is the oxide film itself.

The origin of the inductive loop has often been attributed to surface or bulk relaxation of species in the oxide layer.[36] The LF inductive loop may be related to the relaxation process obtained by adsorption and incorporation of sulphate ions, oxide ions, and charged intermediates on and into the oxide film.[33] The second capacitive loop observed at LF values could be assigned to the metal dissolution.[32] The measured values of polarization resistance (R_p) increase with the increasing concentration of DMABT in the solution, indicating the decrease in the corrosion rate for the base metal with increase in DMABT concentration up to critical concentration of the inhibitor. This is in accordance with the observations obtained from potentiodynamic measurements.

However, in the case of Al/SiC composites, the obtained semicircles in absence or in presence of inhibitor are depressed. Deviation of this kind are referred to as frequency dispersion, have been attributed to inhomogeneties of solid surfaces, as the aluminum composite is reinforced with SiC particles. Mansfeld et al.[40−41] have suggested an exponent n in the impedance function as a deviation parameter from the ideal behavior. By this suggestion, the capacitor in the equivalent circuit can be replaced by a so-called constant phase element (CPE) that is a frequency-dependent element and related to surface roughness. The impedance function of a CPE has the following equation:[31]

$$Z_{CPE} = \frac{1}{(Y_o/\omega)^n} \qquad [4]$$

where the amplitude Y_0 and n are frequency independent, and ω is the angular frequency for which $-Z''$ reaches its maximum values, n is dependent on the surface morphology, with values, $-1 \leq n \leq 1$. Y_0 and n can be calculated by the equations proved by Mansfeld et al.[39,40] In the case of base alloy, due to the homogenous surface, frequency dispersion is very less. Therefore the obtained semicircles in the impedance spectra are not depressed.

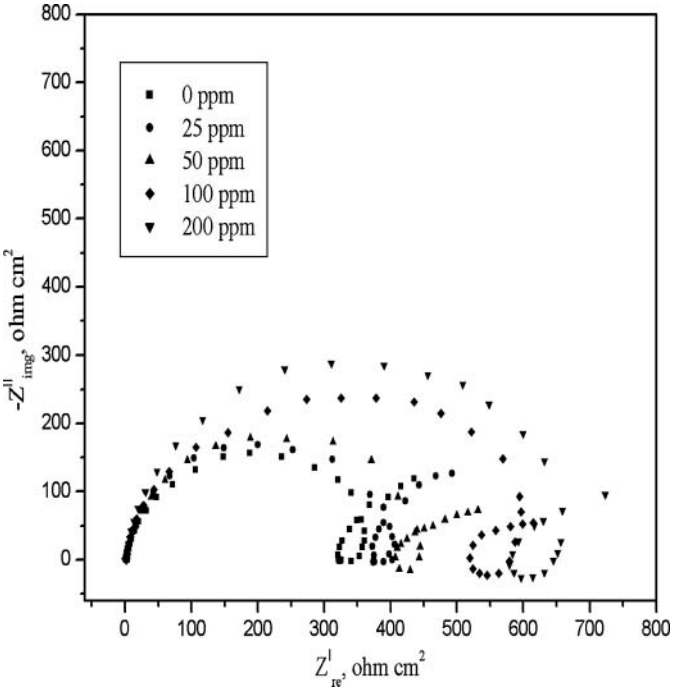

FIG. 4. Nyquist plots of 6061 base alloy in 0.5 M sulfuric acid at 30°C in the presence of different concentrations of DEABT.

TABLE 3
Electrochemical parameters obtained from EIS measurements of 6061 Al-SiC composite and its base alloy at various concentrations of DMABT at 30°C

	Composite				Base alloy			
Conc. of H_2SO_4 (M)	Conc. of inhibitor (ppm)	R_t (Ω cm^2)	CPE (μF cm^{-2})	IE (%)	Conc. of inhibitor (ppm)	R_t (Ω cm^2)	CPE (μF cm^{-2})	IE (%)
0.5	0	93.9	222		0	360.1	27.1	
	50	125.4	199	25	25	451.0	26.1	20
	100	148.5	168	45	50	523.7	26.1	31
	200	221.0	140	58	100	671.5	24.7	46
	400	340.8	120	72	200	799.2	22.3	55
0.25	0	213.0	179		0	456.7	26.4	
	25	279.3	158	23	25	551.1	24.1	17
	50	312.9	132	32	50	682.9	23.7	33
	100	392.7	111	46	100	839.4	21.4	46
	200	617.8	99	67				
0.05	0	401.0	101		0	720.0	16.7	
	10	499.4	79	20	5	862.3	15.0	17
	25	612.9	64	35	10	979.9	13.5	27
	50	884.5	58	55	25	1322.7	12.8	46

An equivalent circuit of five elements depicted in Figure 5a was used to simulate the measured impedance data, as shown in Figure 5b. In this equivalent circuit R_s is the solution resistance and R_t is the charge transfer resistance. $R_L$and L represent the inductive elements. This also consists of constant phase element, CPE (Q) in parallel to the parallel resistors R_t and R_L, and the later is in series with the inductor L. he polarization resistance R_p can be calculated from:[5]

$$R_p = \frac{R_L \times R_t}{R_L + R_t} \quad [5]$$

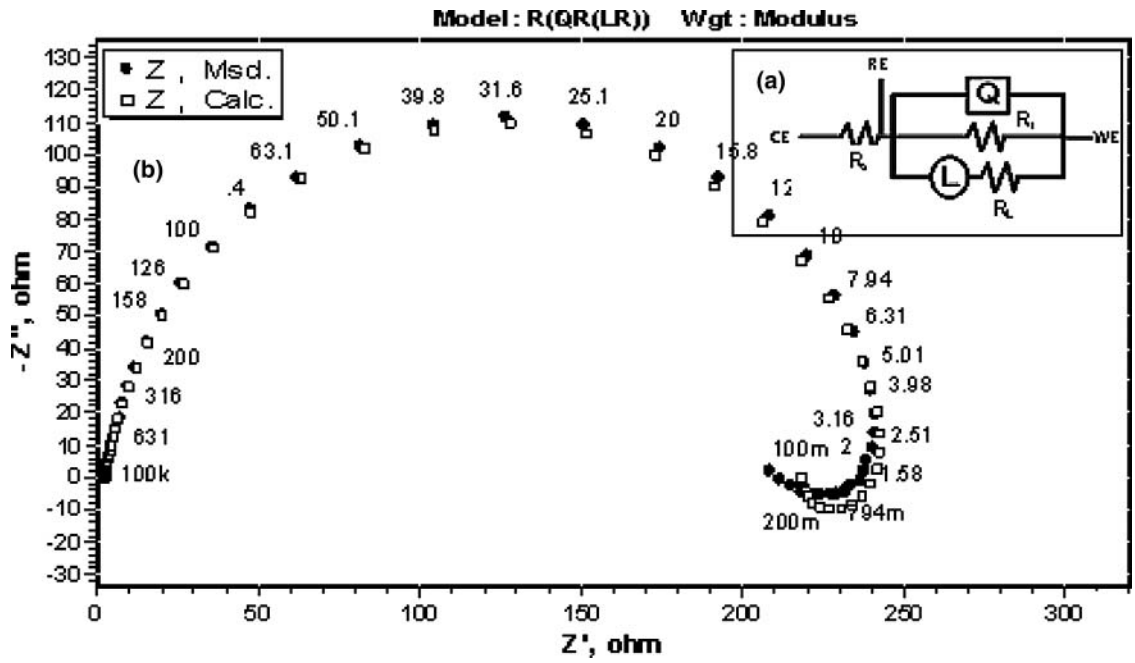

FIG. 5. The equivalent circuit model used to fit the experimental data of the composite.

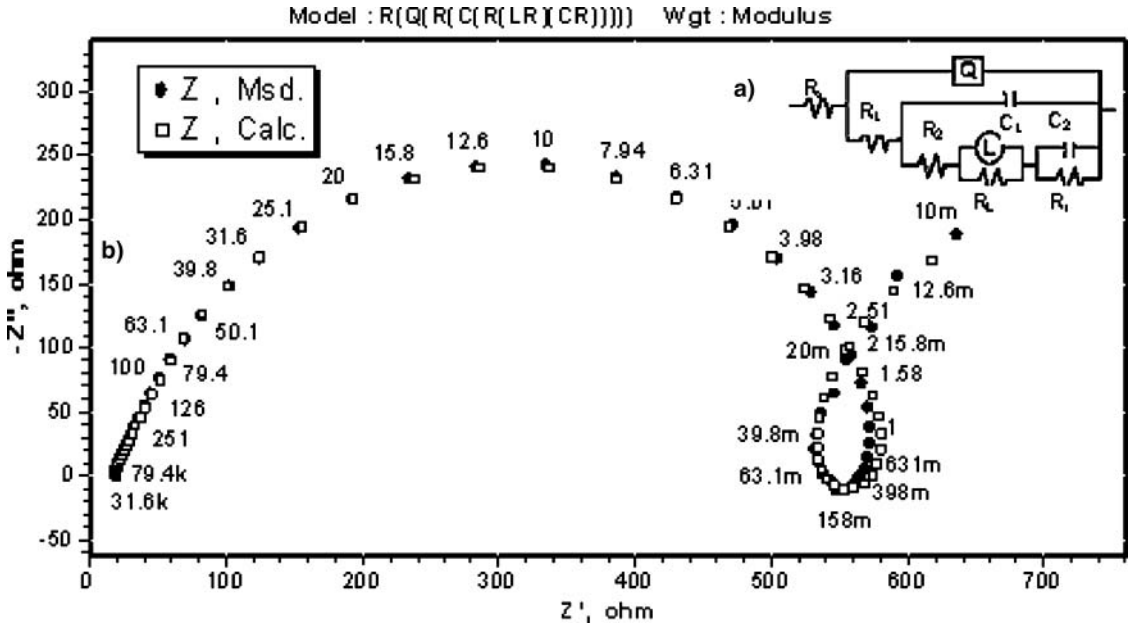

FIG. 6. The equivalent circuit model used to fit the experimental data of the base alloy.

An equivalent circuit of nine elements depicted in Figure 6a was used to simulate the measured impedance data of the base alloy, as shown in Figure 6b. In this equivalent circuit R_s is the solution resistance and R_t is the charge transfer resistance. $R_L$and L represent the inductive elements. This also consists of constant phase element; CPE (Q) in parallel to the series capacitors C_1, $C_2$and series resistors R_1, R_2, R_L and R_t. R_L is parallel with the inductor L. The polarization resistance R_p and double layer capacitance C_{dl} can be calculated from equations (6) and (7):

$$R_p = R_L + R_t + R_1 + R_2 \quad [6]$$

$$C_{dl} = C_1 + C_2 \quad [7]$$

Since R_p is inversely proportional to the corrosion current and it can be used to calculate the inhibition efficiency from the relation,

$$IE\,\% = \left(\frac{R'_p - R_p}{R'_p}\right) \times 100 \quad [8]$$

where R'_p and R_p are the polarization resistances in the presence and absence of inhibitors.

The Bode plots for 6061 Al/ SiC composite and its base alloy with and without inhibitor, obtained at OCP, are presented in Figures 7 and 8. It is apparent that, in the case composite, the phase angle maxima are quite broad after addition of DMABT where as there is no significant change was observed for the base alloy.

It is seen from Table 3 that R_s (solution resistance) remains almost constant, with and without addition of DMABT for both the composite and its base alloy. It was also observed that the value of constant phase element, Q, decreases, while the values of R_t increase with increasing concentration of DMABT, indicating that the inhibition efficiency increases with the increase in concentration of DMABT. The double layer between the charged metal surface and the solution is considered as an electrical capacitor. The adsorption of DMABT on the aluminum surface decreases its electrical capacity because they displace the water molecules and other ions originally adsorbed on the surface. The decrease in this capacity with increase in DMABT

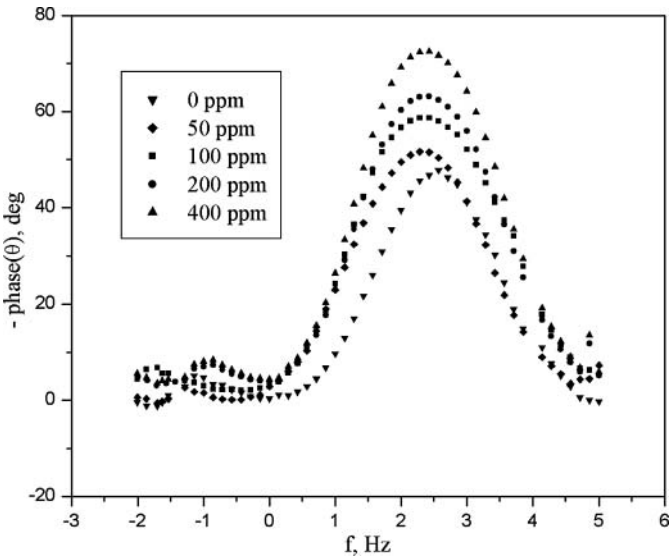

FIG. 7. Bode plots of 6061 composite in 0.5 M sulfuric acid at 30°C in the presence of different concentrations of DMABT.

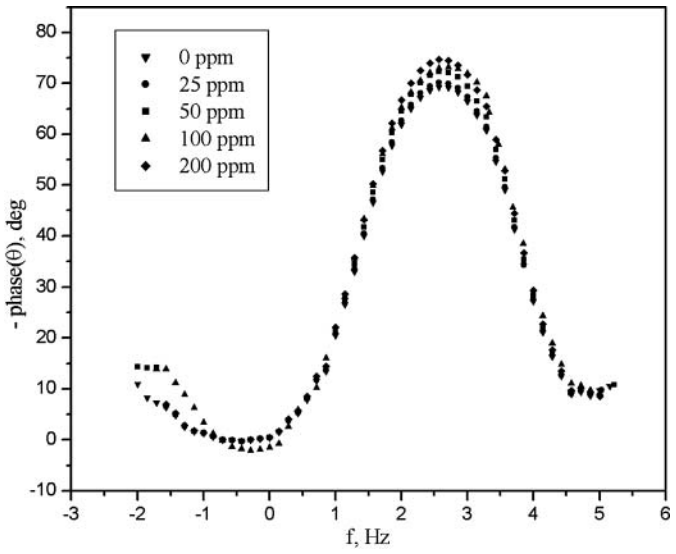

FIG. 8. Bode plots of 6061 base alloy in 0.5 M sulfuric acid at 30°C in the presence of different concentrations of DMABT.

concentrations may be attributed to the formation of a protective layer on the electrode surface. The thickness of this protective layer increases with increase in inhibitor concentration up to their critical concentration and then decreases. The obtained CPE (Q) values decrease noticeably with increase in the concentration of DMABT. In the case of composites, adsorption of negatively charged heteroatoms and π electrons of the benzene ring of DMABT at the Al/SiC interface occurs to a better extent than the base alloy (Q is inversely proportional to the thickness of the surface film or protective layer). In the case of base alloys due to the homogenous surface, frequency dispersion is very less. Therefore the obtained semicircles in the impedance spectra are not depressed. Significant change in the CPE values of the base alloy is not observed after the addition of an inhibitor.

A comparison of the maximum attainable inhibiting efficiencies obtained using a.c and d.c methods are listed in Table 4 for both the composite and the base alloy in 0.5 M sulfuric acid at different temperatures. The results show that the inhibition efficiencies determined by the two techniques are in acceptable level of good agreement. Similar level of agreement was observed at other two concentrations of the acid mixtures also. Though the inhibition efficiencies obtained at lower temperatures (30°C, 35°C, 40°C) are quite high, it is bit lower at higher temperatures (45°C and 50°C). Tables 2, 3 and 4 also reveal that the optimum concentration of DMABT required for maximum efficiency is higher for the composite than for the base alloy. Above the optimum concentration of DMABT given in the tables, there was no appreciable increase in the inhibition efficiencies. The inhibition efficiencies are as high as 71% for the composite and 52% for the base alloy in 0.5 M sulfuric acid solution, but the values are 52% and 43% in 0.05 M sulfuric acid solution.

Effect of Temperature and Activation Parameters of Inhibition Process

The results obtained indicate that the rates of aluminum corrosion in absence and presence of DMABT increased with temperature while the inhibition efficiency decreased. This may be attributed to the higher dissolution rates of aluminum at elevated temperature and a possible desorption of adsorbed inhibitor due to increased solution agitation resulting from higher rates of hydrogen gas evolution, which may also reduce the ability of the inhibitor to be adsorbed on the metal surface. Such a behavior, observed in both samples, suggests physical adsorption of the DMABT on the corroding aluminum surface.[42–44]

Plot of ln(corrosion rate) vs. 1/T for 6061 Al composite in 0.5 M sulfuric acid in absence and presence of various concentrations of DMABT is shown in Figure 9. As shown from this figure, straight lines were obtained according to Arrhenius – type equation:

$$\ln(\text{corrosion rate}) = A - \frac{E_a}{RT} \qquad [9]$$

TABLE 4
Maximum inhibitor efficiency obtained in 0.5 M sulfuric acid solution at different temperatures

Temperature of the medium (°C)	Composite			Base alloy		
	Optimum inhibitor concentration (ppm)	Inhibition efficiency (%)		Optimum inhibitor concentration (ppm)	Inhibition efficiency (%)	
		Tafel method	EIS method		Tafel method	EIS method
30	400	71	72	200	52	54
35	400	67	70	200	51	52
40	400	56	58	200	47	49
45	400	48	50	200	42	45
50	400	44	47	200	38	41

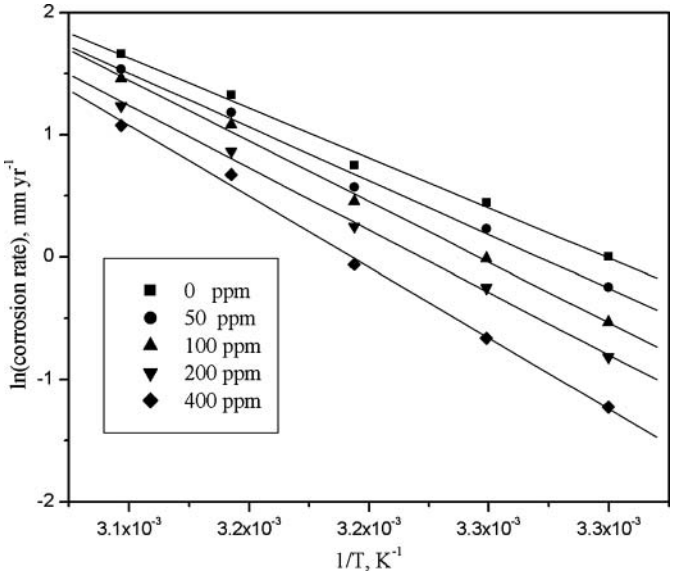

FIG. 9. Arrhenius plots for the composite in 0.5 M sulfuric acid at different concentrations of DMABT.

where A is constant depends on metal type and electrolyte, E_a is the apparent activation energy, R is the universal gas constant, and T is the absolute temperature. Similar plots are obtained for the base alloy also.

Plot of ln(corrosion rate /T) vs 1/T for both the samples of aluminum 6061 in 0.5 M sulfuric acid in absence and presence of various concentrations of DMABT is shown in Figure 10. As shown from this figure, straight lines were obtained according to transition state equation:

$$\text{Corrosion rate} = \frac{RT}{Nh} e^{\frac{\Delta S^{\#}}{R}} e^{\frac{\Delta H^{\#}}{RT}} \quad [10]$$

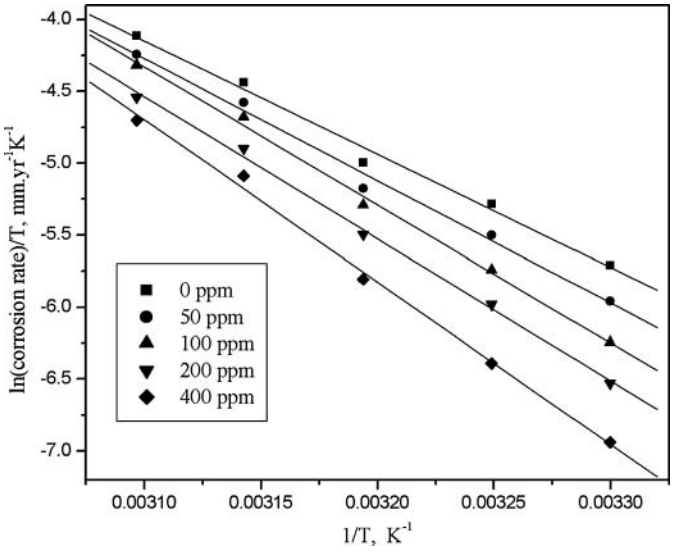

FIG. 10. ln(corrosion rate/T) vs. 1/T for composite in 0.5 M sulfuric acid at different concentrations of DMABT.

where h is Planck's constant, N is Avogadro's number, $\Delta H^{\#}$ is the activation enthalpy, and $\Delta S^{\#}$ is the activation entropy. The calculated values of apparent activation energy, E_a, activation enthalpies, $\Delta H^{\#}$, and activation entropies, $\Delta S^{\#}$ are given in Tables 5 and 6. These values indicate that the presence of inhibitor increases the activation energy, E_a, and the activation enthalpies, $\Delta H^{\#}$. The increase in the activation energies with increasing concentration of the inhibitor is attributed to an appreciable increase in the adsorption process of the inhibitor on the metal surface with increase in the concentration of inhibitor.

The addition of inhibitor modified the values of Ea; this modification may be attributed to the change in the mechanism of the corrosion process in the presence of adsorbed inhibitor molecules.[45] The lower value of the activation energy of the process in the presence of inhibitors when compared to that in its absence is attributed to its chemisorption, while the opposite is the case with physical adsorption.[46–47] In the case of both samples of aluminum, the inhibition efficiency decreases with increase in temperature, which indicates desorption of inhibitor molecule.[48]

The values of $\Delta S^{\#}$ are higher for inhibited solutions than that for the uninhibited solutions. This suggested that an increase in randomness occurred on going from reactants to the activated complex. This might be the results of the adsorption of organic inhibitor molecules from the acidic solution, which could be regarded as a quasi-substitution process between the organic compound in the aqueous phase and water molecules at electrode surface.[49] In this situation, the adsorption of organic inhibitor is accompanied by desorption of water molecules from the surface. Thus, the increase in entropy of activation can be attributed to the increasing in solvent entropy.[50]

Adsorption Isotherm

In order to understand the mechanism of corrosion inhibition, the adsorption behavior of the organic adsorbate on the aluminum surface must be known. The degree of surface coverage (θ) for different concentration of inhibitor was evaluated from potentiodynamic polarization measurements. A correlation between θ and inhibitor concentration in the corrosive medium can be represented by the Langmuir adsorption isotherm.

$$\frac{\theta}{(1-\theta)} = K_{ads}\, C \quad [11]$$

where K_{ads} is the equilibrium constant of the inhibitor adsorption process and C is the inhibitor concentration.

A straight line was obtained on plotting C/θ against C, suggesting that the adsorption of the compound on aluminum surface follows Langmuir adsorption isotherm model. The slopes are close to 1, and the strong correlation ($R^2 > 0.99$) proved that the adsorption of DMABT on the metal surface obeyed to the Langmuir's adsorption isotherm. The high values of K for the studied inhibitor indicate strong adsorption of inhibitor

TABLE 5
Activation parameters of the corrosion of 6061 Al-SiC composite in absence and presence of different concentrations of DMABT

	Medium													
	0.5 M H_2SO_4 Inhibitor concentration (ppm)					0.25 M H_2SO_4 Inhibitor concentration (ppm)					0.05 M H_2SO_4 Inhibitor concentration (ppm)			
Activation parameters	0	50	100	200	400	0	25	50	100	200	0	10	25	50
E_a (kJ mol^{-1})	68.8	74.7	80.3	86.5	98.4	66.0	74.8	76.7	77.2	79.5	53.0	58.4	60.9	67.5
$\Delta H^{\#}$ (kJ mol^{-1})	65.5	71.3	76.8	83.1	94.9	63.4	72.2	74.1	74.9	76.9	50.3	55.8	58.3	64.9
$\Delta S^{\#}$ (J K^{-1} mol^{-1})	82.7	99.7	114.7	133.5	168.7	69.0	95.6	100.6	102.1	105.6	22.4	38.2	41.6	64.8

on the alloy surface. Adsorption isotherms for different concentrations of DMABT, on the surface of 6061 Al- SiC composite in 0.5 M sulfuric acid at different temperatures are shown in Figure 11. Similar plots were also obtained for the base alloy.

The free energy of adsorption, ΔG^0_{ads} was calculated using the relation,

$$\Delta G^{\circ} = -\mathrm{RT}\ln\left[\frac{55.5\,\theta}{C(1-\theta)}\right] \qquad [12]$$

where C is the concentration of the inhibitor expressed in mole dm^{-3}. The calculated values of ΔG^0_{ads} for DMABT on the composite and the base alloy were in the range of -27.11 to -28.59 kJ $mol^{-1}$and -27.00 to -28.83 kJ mol^{-1}, respectively. The negative values of ΔG^0_{ads} suggest the spontaneous adsorption of DMABT on the composite and base alloy surfaces. Since the values of ΔG^0_{ads} of -40 kJ mol^{-1} is usually accepted as threshold value between chemisorption and physisorption, the obtained values of the ΔG^0_{ads} may be indicative of both physical and chemical process.[51]

The enthalpy of adsorption was calculated using rearranged form of Gibbs – Helmholtz equation

$$\Delta G^0_{ads} = \Delta H^0_{ads} - \mathrm{T}\Delta S^0_{ads} \qquad [13]$$

The variation of ΔG^0_{ads} with T gives a straight line with an intercept that equals ΔH^0_{ads} (Figure 12). Figure shows the good dependence of ΔG^0_{ads} on T, indicating good correlation among thermodynamic parameters. The thermodynamic data obtained for DMABT adsorbed on aluminum composite and base alloy are listed in Table 7. The negative sign of ΔH^0_{ads} in sulfuric acid solution indicates that the adsorption of inhibitor molecule is an exothermic process. Generally, an exothermic adsorption process signifies either physisorption or chemisorptions, while endothermic process is attributable to chemisorptions.[52] Typically, the enthalpy of physisorption process is lower than that 41.86 kJ mol^{-1} while the enthalpy of chemisorptions process approaches 100 kJ mol^{-1}.[53] In the present study, the absolute value of enthalpy is -62.45 kJ mol^{-1} and -50.02 kJ mol^{-1} for the composite and base alloy, respectively, which is an

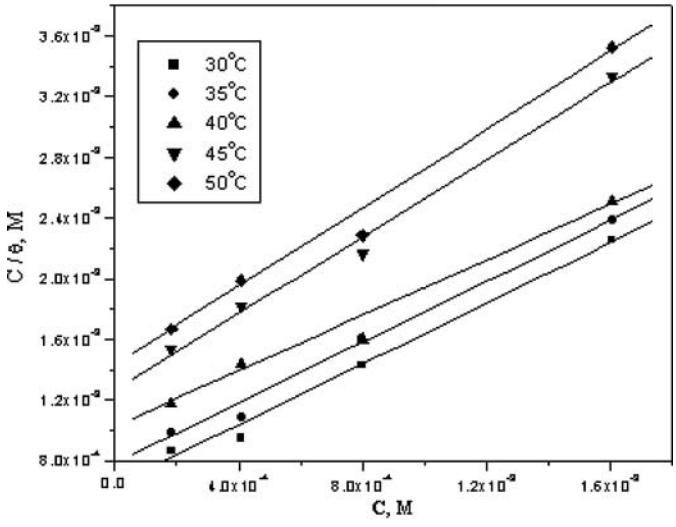

FIG. 11. Langmuir adsorption isotherm for the adsorption of DMABT on the composite.

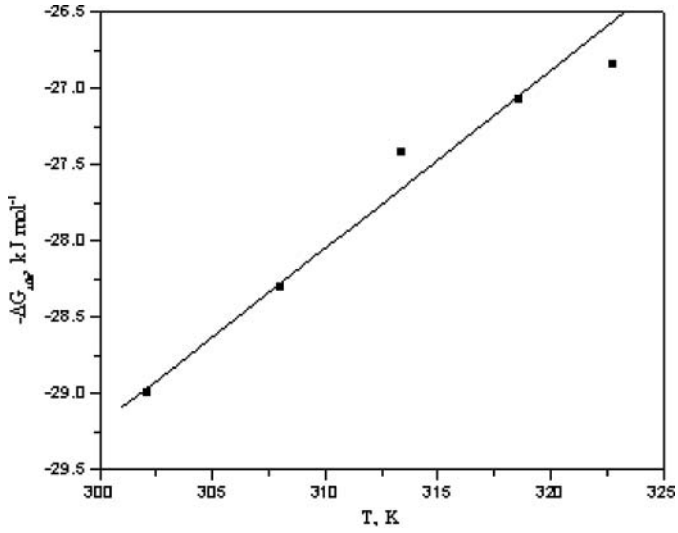

FIG. 12. Plot of ΔG^0 vs. T for the composite.

TABLE 6
Activation parameters of the corrosion of 6061 Al base alloy in absence and presence of different concentrations of DMABT

	Medium												
	0.5 M H_2SO_4 Inhibitor concentration (ppm)					0.25 M H_2SO_4 Inhibitor concentration (ppm)				0.05 M H_2SO_4 Inhibitor concentration (ppm)			
Activation parameters	0	25	50	100	200	0	25	50	100	0	5	10	25
E_a (kJ mol^{-1})	58.7	61.1	61.3	69.6	76.6	63.9	65.0	71.1	72.7	59.8	63.1	64.5	65.1
$\Delta H^{\#}$ (kJ mol^{-1})	56.2	58.6	59.6	67.1	74.2	61.2	62.4	68.5	70.1	57.2	60.5	61.9	62.5
$\Delta S^{\#}$ (J K^{-1} mol^{-1})	40.7	47.4	51.5	71.5	93.1	54.7	56.5	74.8	78.1	37.4	45.7	50.7	54.3

intermediate case. The ΔS^0_{ads} value is large and negative, indicating that an ordering takes place when the inhibitor gets adsorbed on the metal alloy surface.[54]

Mechanism of Inhibition

The corrosion inhibition property of DMABT through adsorption on the surface of the composite or the base alloy can be attributed to the presence of electronegative elements like nitrogen and sulfur, and also to the presence of π electrons on the benzene ring. The metal surface in contact with a solution is charged due to the electric field that emerges at the interface. This can be determined, according to Antrapov,[55] by comparing the zero charge potential and the rest potential of the metal in the corresponding medium. The value of pH_{Zch}, which is defined as the pH at a point of zero charge is equal to 9.1 for aluminum.[56] So aluminium is positively charged in highly acidic medium, as the ones used in this investigation. Therefore, sulphate ions and DMABT can be adsorbed on aluminum surface via their negative centres. Also, DMABT can be protonated in the highly acidic solution used in the investigation. The mechanism of adsorption of protonated DMABT can be predicted on the basis of the mechanism proposed for the corrosion of aluminum in hydrochloric acid.[57] According to this mechanism, anodic dissolution of Al follows steps

$$Al + Cl^- \rightleftharpoons Al\,Cl^-_{(ads)} \quad [14]$$

$$Al\,Cl^-_{(ads)} + Cl^- \rightarrow Al\,Cl^+_2 + 3e^- \quad [15]$$

The cathodic hydrogen evolution is according to the following steps

$$H^+ + e^- \rightarrow H_{(ads)} \quad [16]$$

$$H_{(ads)} + H_{(ads)} \rightarrow H_2 \quad [17]$$

In acidic solution, all the nitrogen atoms including secondary amino group can be protonated easily because they are all planar and having greater electron density. The protonated molecules can get adsorbed on the cathodic sites of aluminum in competition with the hydrogen ions (equation 16). Co-ordinate covalent bond formation between electron pairs of unprotonated S atom and metal surface can take place. Further, DMABT molecules are chemically adsorbed due to interaction of π–orbitals with metal surface following deprotonization step of the physically adsorbed protonated molecules.

As observed from Tables 2 and 3, the corrosion rate as well as the inhibition efficiency increases with increase in sulfuric acid concentration, and is maximum in 0.5 M solution. The

TABLE 7
Thermodynamic parameters for the adsorption of DEABT on Al composite and base alloy in a mixture of 0.5 M sulfuric acid at different temperatures

	Composite				Base alloy			
Temperature (K)	K M^{-1}	ΔG^0_{ads} (kJ mol^{-1})	ΔH^0_{ads} ((kJ mol^{-1})	ΔS^0_{ads} (J $mol^{-1}K^{-1}$)	K M^{-1}	ΔG^0_{ads} (kJ mol^{-1})	ΔH^0_{ads} ((kJ mol^{-1})	ΔS^0_{ads} (J $mol^{-1}K^{-1}$)
303	1519.7	−28.59			1782.1	−28.83		
308	1223.6	−28.21			1563.0	−28.51		
313	970.9	−27.95	−62.45	−118.8	1478.5	−28.45	−50.02	−95.3
318	793.7	−27.32			1399.0	−27.50		
323	694.4	−27.11			1100.2	−27.00		

observations can be explained by the above adsorption mechanism. The increase in the extent of adsorption of the inhibitor on the alloy surface and in turn the increase in the inhibitor efficiency can be attributed to the following two facts:

- The increase in the concentration of the acid increases the extent of protonation of the inhibitor molecules, thereby facilitating their adsorption on the cathodic sites.
- With the increase in the concentration of the acid, the anion of the acid (SO_4^{2-}) adsorb physically on the positively charged metal surface, giving rise to a net negative charge on the metal surface.[21] This further facilitates the adsorption of protonated inhibitor molecules.

In the present case, the value of ΔG^0_{ads} is -32.57 kJ mol^{-1} to -33.72 kJ mol^{-1}, hence, indicating that the adsorption of DMABT on the surface of aluminum involves both physical and chemical process. But, as can be seen from Table 7, the values of ΔG^0_{ads} decreased with increasing temperature, indicating that adsorption of DMABT is not favored at higher temperature. This also supports the fact that DMABT is adsorbed predominantly by physisorption on the surface of aluminum composite.

Scanning Electron Microscopy

In order to evaluate the effect of corrosion on the surface morphology of the composite and the base alloy, SEM analysis was carried out on the samples subjected to corrosion in acid mixture containing 0.5 M sulfuric acid in the presence and absence of the inhibitors. Figure 13 shows cavities formed due to detachment of SiC particle from the composite when exposed to the acid mixture medium. This may be attributed to the corrosion at the interface between the particle and matrix due to the galvanic action, with the particle acting as a cathodic site

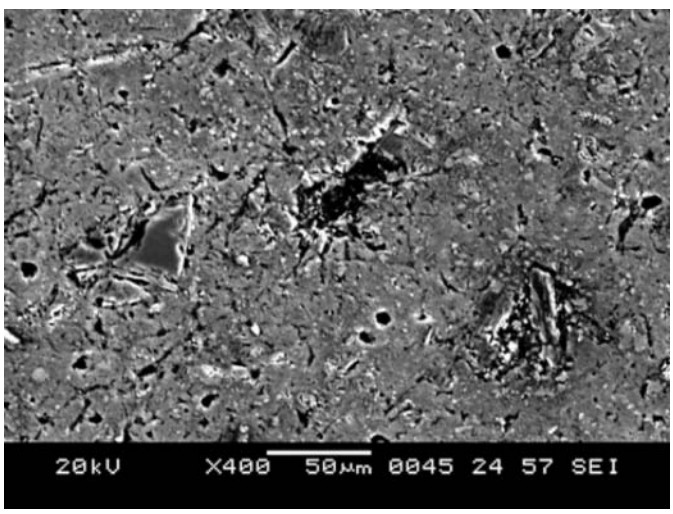

FIG. 13. SEM image of the surface of composite after immersion for 2h in 0.5 M H_2SO_4at 30°C in the absence of DMABT.

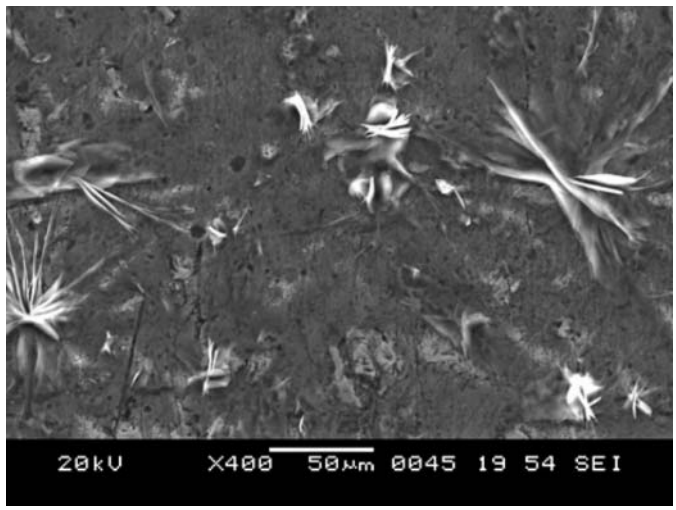

FIG. 14. SEM image of the surface of composite after immersion for 2h in 0.5 M H_2SO_4at 30°C in presence of 400 ppm of DMABT.

and resulting in the detachment of the particle from the matrix. Figure 14 shows more or less smooth surfaces of the composite without pits in the presence of inhibitors.

CONCLUSIONS

1. DMABT acts as a good corrosion inhibitor for 6061 Al- 15 vol. pct. $SiC_{(p)}$ composite and its base alloy in sulfuric acid medium.
2. Corrosion inhibition efficiency of DMABT increases with increasing concentration of inhibitor up to critical concentration.
3. DMABT behaves as cathodic type inhibitor.
4. Inhibition efficiency of DMABT on aluminium composite is more than that of its base alloy.
5. Inhibition efficiency of DMABT on aluminum composite and its base alloy increases with increase in concentration of sulfuric acid and decreases with increase in temperature from 30°C–50°C.
6. Inhibitor obeys Langmuir's model of adsorption, and the adsorption is predominantly through physisorption.
7. The adsorption process is spontaneous and exothermic process accompanied by an increase of entropy.

REFERENCES

1. Sanders Jr., T.H.; Starke Jr., E.A. Influence of heat treatment on the coefficient of thermal expansion of Al (6061) based hybrid composites. *Proceedings of the Fifth International Conference on Al–Lithium alloys*, Materials & Composites Engineering Publications Ltd., Birmingham, UK., 1–40, **1989**.
2. Monticelli, C.; Zucchi, F.; Brunoro, G.; Trabanelli, G. Corrosion and corrosion inhibition of alumina particulate/aluminum alloys metal matrix composites. *J. Appl. Electrochem*. **1997**, *27*(2), 325.
3. Pardo, A.; Merino, M.C.; Merino, S.; Viejo, F.; Carboneras, M.; Arrabal, R. Influence of reinforcement proportion and matrix composition on pitting corrosion behavior of cast aluminum matrix composites (A 3xxxx/SiCp). *Corros. Sci*. **2005,** *47*(6), 1750.

4. Da Costa, C.E.; Velasco, F.; Toralba, J.M. Aluminum powder metallurgy: Develop and improve their alloys and composites. *Rev. Metal. Madrid*. **2000**, *36*, 179.
5. Rohatgi, P.K. Cast aluminium–matrix composites for automotive applications. *JOM*. **1991**, *43*(4), 10.
6. Pardo, A.; Merino, M.C.; Merino, S.; Lopez, M.D.; Viejo, F.; Carboneras, M. Influence of reinforcement proportion and matrix composition on pitting corrosion behavior of cast aluminium matrix composites in a humid environment. *Mater.Corros*. **2003**, *54*(5), 311.
7. Peel, C.J.; Moreton, R.; Gregson, P.J.; Hunt, E.P. Influence of heat treatment on the coefficient of thermal expansion of Al (6061) based hybrid composites. *Proceedings of the XII International Conference on Society of Advanced Material and Process Engineering*, SAMPE, Covina, CA. **1991**, pp. 189.
8. Hutchings, I.M.; Wilson, S.; Alpas, A.T.; Clyne, T.W. (ed.). Wear of aluminium based composites. *Comprehensive Composite Materials*, Vol.3; Elsevier Science Ltd: UK., **2000**, 501–505.
9. Aylor, D.M. *Corrosion of Metal Matrix Composites*, *Metals Hand Book*, Vol.13, Ninth Edition; ASM, **1987**, pp. 859.
10. Trowsdate, A.J.; Noble, B.; Haris, S.J.; Gibbins, I.S.R.; Thomson, G.E.; Wood, G.C. The influence of silicon carbide reinforcement on the pitting behavior of aluminum. *Corros. Sci.* **1996**, *38*(2), 177.
11. Bentiss, F.; Treisnel; Lagrence, M. Inhibitor effects of triazole derivatives on corrosion of mild steel in acidic media. Br. *Corros. J*. **2000**, *35*, 315.
12. Rao, S.A.; Padmalatha; Nayak, J.; Shetty, A.N. 3-Methyl-4- amino-5-mercapto-1,2,4-triazole as inhibitor of corrosion of 6061 Al- 15 vol.pct. SiC(p) composite. *J. Met. and Mat. Sci*. **2005**, *47*(1), 51–57.
13. Desai, M.N.; Rana, S.S.; Gandhi M.H.; C.B. Snah. Corrosion inhibitors for aluminium and aluminum –base alloys. *Anticorrosion Methods and Materials* **1971**, *18*(5), 4.
14. Desai, M.N.; Rana, S.S.; Gandhi, M.H.; Snah, C.B. Corrosion inhibitors for copper. *Anticorrosion Methods and Materials* **1971**, *18*(2), 19.
15. Muller, B. Citric acid as corrosion inhibitor for aluminium pigment. *Corros. Sci.* **2004**, *46*, 159–167.
16. Putilova, I.N.; Balezin S.A.; Arannik, B. *Metallic Corrosion Inhibitors*; Pergamon: Oxford, **1960**.
17. Trabanelli, G.; Montecelli, C.; Grassi, V.; Frignani, A. Electrochemical study on inhibitors of rebar corrosion in carbonated concrete. *J. Cem. Concr. Res*. **2005**, *35*(9), 1804.
18. Rozerfeld, I.L. *Corrosion Inhibitors*; McGraw Hill: New York, **1981**.
19. Nathan, C.C. *Corrosion Inhibitors*; NACE: Houston, **1973**.
20. Hunkeler, F.; Bohni, H. Inhibition of pit initiation and pit growth on aluminum. *Workstoffe u. Korrosion* **1983**, *34*, 68.
21. Noor, E.A. Evaluation of inhibitive action of some quaternary N-heterocyclic compounds on the corrosion of Al–Cu alloy in hydrochloric acid. *Mater. Chem. Phys*. **2009**, *114*, 533–541.
22. Arab, S.T. Inhibition action of thiosemicarbazone and some of its ρ- substituted compounds on the corrosion of iron base metallic glass alloy in 0.5M H_2SO_4 at 30°C. *Materials Research Bulletin* **2008**, *43*(3), 510.
23. Abd El-Nabey, B.A.; Khamis, E. Effect of temperature on the inhibition of the acid corrosion of steel by benzaldehyde thiosemicarbazone: Impedance measurements. *Surf. and Coat. Tech.* **1986**, *28*, 83.
24. Shah, P.T.; Daniels, T.C. Synthesis and characterization of lanthanide(III) complexes with N, N-diethylaminobenzaldehyde thiosemicarbazone. *Rev. Trav. Chim*. **1950**, *69*, 1545.
25. Bethencourt, M.; Botana, F.J.; Cauqui, M.A.; Marcos, M.; Rodriguez, M.A. Protection against corrosion in marine environments of AA5083 Al–Mg alloy by lanthanide chlorides. *J. Alloys Compd*. **1997**, *250*, 455.
26. Abdel Rahim, S.S.; Hassan, H.H.; Amin, M.A. The corrosion inhibition study of sodium dodecyl benzene sulphonate to aluminium and its alloys in 1.0 M HCl solution. *Mater. Chem. Phys*. **2002**, *78*(2), 337.
27. Aramaki, K. Effects of organic inhibitors on corrosion of zinc in an aerated 0.5 M NaCl solution. *Corros. Sci*. **2001**, *43*(10), 1985–2000.
28. el Kadher, A.; El Warraky, J.M.; Abd el Aziz, A.M. Corrosion inhibition of mild steel by sodium tungstate in neutral solution. *Br. Corr. J*. **1998**, *33*(2), 139.
29. Khaled, K.F.; Al-Qahtani, M.M. The inhibitive effect of some tetrazole derivatives towards Al corrosion in acid solution: Chemical, electrochemical and theoretical studies. *Mater.Chem. Phys.* **2009**, *113*(1), 150–158.
30. Sayed, S.; Rehim, A.; Hamdi Hassan, H.; Mohammed, A.A. Corrosion and corrosion inhibition of Al and some alloys in sulphate solutions containing halide ions investigated by an impedance technique**.** *App. Surf. Sci*. **2002**, *187*(3–4), 279–290
31. Lenderink Linden, H.J.W.; De Wit, M.V.D. Corrosion of aluminium in acidic and neutral solutions. *Electrochem. Acta* **1993**, *38*(14), 1989–1992.
32. Wit, J.H.; Lenderink, H.J.W. Electrochemical impedance spectroscopy as a tool to obtain mechanistic information on the passive behavior of aluminum. *Electrochim. Acta*. **1996**, *41(7-8),* 1111–1119.
33. Bessone, J.; Mayer, J.B.; Jutner, C.; Lorenz, W.J. Ac impedance measurements on aluminium barrier type oxide films. *Electrochim Acta.* **1983**, *28*(2), 171.
34. Frers, S.E.; Stefenel, M.M.; Mayer, C.; Chierchie, T. AC-Impedance measurements on aluminium in chloride containing solutions and below the pitting potential. *J. Appl. Electrochem*. **1990**, *20*(6), 996–999.
35. Metikos-Hukovic, M.; Babic R.; Grubac, Z. Corrosion protection of aluminium in acidic chloride solutions with nontoxic inhibitors. *J. Appl. Electrochem*. **1998**, *28*(4), 433–469.
36. Brett, C.M.A. The application of electrochemical impedance techniques to aluminium corrosion in acidic chloride solution. *J. Appl. Electrochem*. **1990**, *20*(6), 1000–1003.
37. Lee E.J.; Pyun. The effect of oxide chemistry on the passivity of aluminium surfaces. *Corros. Sci*. **1995**, *37*(1), 157–168.
38. Brett, C.M.A. On the electrochemical behavior of aluminum in acidic chloride solution. *Corros. Sci*. **1992**, *33*(2), 203–210.
39. Aytac, A.; Ozmen, U.; Kabasakaloglu, M. Investigation of some Schiff base as acidic corrosion of AA 3102. *Mater.Chem. Phys.* **2005**, *89*(1), 176–181.
40. Mansfeld, F.; Lin, S.; Kim, S.; Shih, H. Pitting and surface modification of SiC/Al. *Corros. Sci.* **1987**, *27*(9), 997.
41. Mansfeld, F.; Lin, S.; Kim, S.; Shih, H. Electrochemical impedance spectroscopy as a monitoring tool for passivation and localised corrosion. *West u Korros*. **1988**, *39*(11), 487.
42. Migahed, M.A. Electrochemical investigation of the corrosion behavior of mild steel in 2 M HCl solution in presence of 1-dodecyl-4-methoxy pyridinium bromide. *Mater.Chem*. **2005**, *93*(1), 48–53.
43. Abdallah, M. Antibacterial drugs as corrosion inhibitors for corrosion of aluminium in hydrochloric solution. *Corros. Sci*. **2004**, *46*(8), 1981–1996.
44. Oguzie, E.E. Corrosion inhibition of aluminium in acidic and alkaline media by *Sansevieria trifasciata* extract. *Corros. Sci*. **2007**, *49*(3), 1527–1539.
45. Mernari, B.; Elkadi, L.; Kertit, S. 2,5 bis(2-thienyl)-1,3,4-oxadiazole as corrosion inhibitor of mild steel in acidic media. *Bull. Electrochem*. **2001**, *17*, 115.
46. Szauer, T. Brandt, A. Adsorption of oleates of various amines on iron in acidic solution. *Electrochim. Acta*. **1981**, *26*, 1253.
47. El Sherbini, E.F. Effect of some ethoxylated fatty acids on the corrosion behaviour of mild steel in sulfuric acid solution. *Mat. Chem. Phys*. **1999**, *60*, 286
48. Kumar Singh, A.; Quraishi, M.A. Effect of Cefazolin on the corrosion of mild steel in HCl solution. *Corros Sci*. **2010**, *52*, 156.
49. Sahin, M.; Bilgic, S.; Yilmaz, H. The inhibition effects of some cyclic nitrogen compounds on the corrosion of the steel in NaCl mediums. *Appl. Surf. Sci*. **2002**, *195*, 17.
50. Ateya, B.; El-Anadouli, B.E.; El-Nizamy, F.M. The effect of thiourea on the corrosion kinetics of mild steel in H_2SO_4. *Corros. Sci*. **1984**, *24*(6), 497–507.
51. Geler, E.; Azambuja, D.S. Corrosion inhibition of copper in chloride solutions by Pyrazole. *Corros. Sci.* **2000**, *42*(4), 631–643.

52. Durnie, W. ; De Marco, R. ; Kinsella, B. ; Jefferson, A. A study of adsorption properties of commercial carbon dioxide corrosion inhibitor formulations. *J. Electrochem. Soc*. **2001**, *31*(11), 1221–1226.
53. Martinez, S.; Stern, I. Thermodynamic characterization of metal dissolution and inhibitor adsorption processes in the low carbon steel/mimosa tannin/sulfuric acid system. *Appl. Surf. Sci*. **2002**, *199*(1-4), 83–89.
54. Tao, Z.; Zhang, S.; Li, W.; Hou, B. Corrosion inhibition of mild steel in acidic solution by some oxo-triazole derivatives. *Corros. Sci*. **2009**, *51*(11), 2588–2595.
55. Antropov, L.I.; Makushin, E.M.; Panasenko, V.F. *Metallic Corrosion Inhibitors*; Kiev: Technika, **1981**, pp.182.
56. Tschapek, M.C.; Wasowski, R.M.; Sanchez, T. The p.z.c. and i.e. of γ-Al_2O_3 and TiO_2. *J. Electroanal.Chem*. **1976**, *74*(2), 167–176.
57. Awady, A.A.; Abd. El- Nabey, B.A.; Aziz, S.G. Thermodynamic and kinetic factors in chloride ion pitting and nitrogen donor ligand inhibition of aluminum metal corrosion in aggressive acid media. *J. Chem. Soc. Faraday Trans*. **1993**, *89*, 795–802.